ETH
Eidgenössische Technische Hochschule Zürich
Swiss Federal Institute of Technology Zurich

Seminar for Applied Mathematics SAM

Structure preserving schemes

R. Käppeli and S. Mishra

Research Report No. 2014-02
January 2014

Seminar für Angewandte Mathematik
Eidgenössische Technische Hochschule
CH-8092 Zürich
Switzerland

Volume Title
ASP Conference Series, Vol. **Volume Number**
Author

Structure preserving schemes

Roger Käppeli, Siddhartha Mishra

Seminar for Applied Mathematics (SAM), Department of Mathematics, ETH Zürich, CH-8092 Zürich, Switzerland

Abstract. We present two novel structure preserving numerical schemes for the Euler equations of hydrodynamics. The first method is concerned with the exact preservation of certain hydrostatic equilibria. This is achieved by a hydrostatic preserving reconstruction procedure and a well-balanced discretization of the gravitational source term. The second method treats the deficiency of angular momentum conservation in standard Eulerian Godunov-type numerical schemes. We show the geometric requirements on a scheme that conserves mass, linear momentum, total energy and angular momentum simultaneously. We then present a scheme fulfilling these requirements. The performance of the new structure preserving schemes is illustrated through numerical examples.

1. Introduction

The Euler equations of hydrodynamics express the conservation of mass, linear momentum and total energy (Landau et al. 1991). They are a non-linear system of conservation laws, which feature certain structures in the form of companion laws that are fulfilled at the analytical level. When the system is solved numerically, these companion laws may be violated. The purpose of structure preserving numerical schemes is then to fulfill a discrete form of these companion laws. In the following we will consider two such structures, which are of particular interest for astrophysical numerical simulations.

The first concerns the steady states of the Euler equation with gravity. Of particular interest is the hydrostatic equilibrium case

$$\nabla p = -\rho \nabla \phi, \tag{1}$$

where the pressure gradient is exactly balanced by the gravity force. As astrophysically relevant examples, we mention the simulation of small perturbations on a gravitationally stratified atmosphere such as those arising in exoplanet climate modeling, the simulation of waves in stellar atmospheres and convection in stellar interiors, amongst others.

The numerical approximation of nearly hydrostatic configurations is very challenging since a standard numerical scheme does not necessarily satisfy a discrete version of the above balance. In 2.1 we will present a so-called well-balanced scheme that preserves a discrete version of this subtle balance (up to machine precision). As an example, we compare the performance of the new well-balanced scheme and a standard scheme on the simulation of a polytrope in three dimensions.

The second structure concerns the conservation of angular momentum. The conservation law for the angular momentum density $\mathbf{j} = \mathbf{x} \times \rho \mathbf{v}$ follows by simply taking

the cross product of the position vector $\mathbf{x} = [x, y, z]^T$ and the linear momentum eq. (**??**):

$$\frac{\partial \mathbf{j}}{\partial t} + \nabla \cdot \left[\mathbf{x} \times (\rho \mathbf{v} \otimes \mathbf{v} + p\mathbf{I})\right] = -\rho \mathbf{x} \times \nabla \phi. \tag{2}$$

As it is well known (and proved in 2.2), standard (Eulerian Godunov-type) numerical schemes do not conserve angular momentum. This represents a great flaw of standard schemes since the importance of angular momentum conservation can hardly be overemphasized in many, if not all, astrophysically relevant contexts. In 2.2 we will present a scheme that conserves mass, linear momentum, total energy and angular momentum at the same time.

2. Structure preserving schemes

For the ease of presentation, we consider the Euler equations in two space dimensions

$$\frac{\partial \mathbf{u}}{\partial t} + \frac{\partial \mathbf{F}}{\partial x} + \frac{\partial \mathbf{G}}{\partial y} = \mathbf{S}, \tag{3}$$

where $\mathbf{u} = [\rho, \rho v_x, \rho v_y, E]^T$ are the conserved variables. The flux functions in respective directions and the source term are given by

$$\mathbf{F} = \begin{pmatrix} \rho v_x \\ \rho v_x^2 + p \\ \rho v_y v_x \\ (E+p) v_x \end{pmatrix}, \ \mathbf{G} = \begin{pmatrix} \rho v_y \\ \rho v_x v_y \\ \rho v_y^2 + p \\ (E+p) v_y \end{pmatrix} \text{ and } \mathbf{S} = \begin{pmatrix} 0 \\ -\rho \\ 0 \\ -\rho v_x \end{pmatrix} \frac{\partial \phi}{\partial x} + \begin{pmatrix} 0 \\ 0 \\ -\rho \\ -\rho v_y \end{pmatrix} \frac{\partial \phi}{\partial y}. \tag{4}$$

We will denote by $\mathbf{w} = [\rho, v_x, v_y, p]^T$ the primitive variables.

For simplicity we consider a Cartesian domain $[0, L_x] \times [0, L_y]$ discretized by $N_x \times N_y$ regular cells $C_{i,j} = [x_{i-1/2}, x_{i+1/2}] \times [y_{j-1/2}, y_{j+1/2}]$, $i = 1, ..., N_x$ and $j = 1, ..., N_y$, where $x_{i+1/2} - x_{i-1/2} = \Delta x$ and $y_{j+1/2} - y_{j-1/2} = \Delta y$. A standard semi-discrete scheme for the evolution of the cell-averaged conserved variables $\mathbf{u}_{i,j}$ reads (LeVeque 2002)

$$\frac{\mathrm{d}\mathbf{u}_{i,j}}{\mathrm{d}t} = -\frac{1}{\Delta x}\left(\mathbf{F}_{i+1/2,j} - \mathbf{F}_{i-1/2,j}\right) - \frac{1}{\Delta y}\left(\mathbf{G}_{i,j+1/2} - \mathbf{G}_{i,j-1/2}\right) + \mathbf{S}_{i,j}, \tag{5}$$

where the $\mathbf{F}_{i\pm1/2,j}$ and $\mathbf{G}_{i,j\pm1/2}$ are the numerical fluxes in respective direction and $\mathbf{S}_{i,j}$ is the discretized source term.

We compute the numerical fluxes in two ways. In the classical way, the numerical fluxes are obtained by the (approximate) solution of Riemann problems at the cell interfaces

$$\mathbf{F}_{i+1/2,j} = \mathcal{F}_{i+1/2,j} = \mathcal{F}(\mathbf{w}_{i+1/2-,j}, \mathbf{w}_{i+1/2+,j}) \ , \ \mathbf{G}_{i,j+1/2} = \mathcal{G}_{i,j+1/2} = \mathcal{G}(\mathbf{w}_{i,j+1/2-}, \mathbf{w}_{i,j+1/2+}), \tag{6}$$

where the $\mathbf{w}_{i+1/2\pm,j}$, $\mathbf{w}_{i,j+1/2\pm}$ are the cell interface extrapolated primitive variables in respective direction (computed by some reconstruction procedure, see e.g. (LeVeque 2002)).

As a second way, the numerical fluxes are obtained in a genuinely multidimensional manner as developed by Mishra & Tadmor (2011). The numerical fluxes are

computed by averaging so-called numerical potentials, which are centered at the grid's vertices

$$\mathbf{F}_{i+1/2,j} = \frac{1}{2}\left(\mathbf{\Phi}_{i+1/2,j-1/2} + \mathbf{\Phi}_{i+1/2,j+1/2}\right) \ , \ \mathbf{G}_{i,j+1/2} = \frac{1}{2}\left(\mathbf{\Psi}_{i-1/2,j+1/2} + \mathbf{\Psi}_{i+1/2,j+1/2}\right). \tag{7}$$

We use the following simple definitions for the numerical potentials

$$\mathbf{\Phi}_{i+1/2,j+1/2} = \frac{1}{2}\left(\mathcal{F}_{i+1/2,j} + \mathcal{F}_{i+1/2,j+1}\right) \ , \ \mathbf{\Psi}_{i+1/2,j+1/2} = \frac{1}{2}\left(\mathcal{G}_{i,j+1/2} + \mathcal{G}_{i+1,j+1/2}\right), \tag{8}$$

i.e. simple averages of standard numerical fluxes. The numerical potentials can be obtained in variety of ways and we refer to Mishra & Tadmor (2011) and references therein for further details.

The time integration of eq. (5) can be performed by any suitable explicit or implicit integrator. This ends the general discussion of numerical schemes and the specificities of the respective structure preserving scheme is detailed in the following subsections.

2.1. Well-balanced schemes for the Euler equations with gravity

The stationary state eq. (1) specifies only a mechanical equilibrium, which is incomplete as the density and pressure stratifications are not uniquely determined. Hence, (at least[1]) another state variable is needed (e.g. entropy or temperature) to fully specify the equilibrium. However, arbitrary entropy or temperature profiles are generally physically unstable (Landau et al. 1991). Two relevant classes of physically stable hydrostatic equilibria are characterized by isentropic and isothermal conditions.

An analytical expression for an isentropic hydrostatic equilibrium can easily be constructed. Under the constant entropy assumption and with the thermodynamic relation $\mathrm{d}h = T\mathrm{d}s + \mathrm{d}p/\rho$, where h is the specific enthalpy $h = e + p/\rho$, T the temperature and s the specific entropy, the hydrostatic equilibrium (1) can be integrated to

$$h + \phi = const. \tag{9}$$

Similar consideration for the isothermal hydrostatic equilibrium case lead to $g + \phi = const$, where g is the specific Gibbs free energy.

Standard piece-wise polynomial reconstructions in the conserved $\mathbf{u}$ or primitive $\mathbf{w}$ variables do not preserve a hydrostatic equilibrium discretely. Instead, we build our first order equilibrium preserving reconstruction in the variables $\mathbf{z} = [s, v_x, v_y, h]^T$, i.e. the specific entropy, enthalpy and the velocity.

In the following we focus on the one-dimensional and spatially first order accurate case. A piece-wise constant reconstruction is applied to the specific entropy and the velocity. Then, the specific enthalpy is reconstructed by assuming eq. (9) within the considered cell. As a result, the cell interface extrapolated values of the specific enthalpy are given by

$$h_{i-1/2+} = h_i + \phi_i - \phi_{i-1/2} \quad \text{and} \quad h_{i+1/2-} = h_i + \phi_i - \phi_{i+1/2}, \tag{10}$$

where $\phi_{i\pm1/2}$ is the gravitational potential at the cell interface. If the gravitational potential is a known function, the cell interface value can be directly evaluated $\phi_{i\pm1/2} =$

[1] If the matter composition is not uniform, further variables are needed.

$\phi(x_{i\pm1/2})$. If the gravitational potential is only known discretely, e.g. at cell centers because it is itself obtained numerically by solving the Poisson equation in the case of self-gravity, a continuous interpolation[2] procedure is needed. In the case of a uniform mesh, it is simply given by the average $\phi_{i\pm1/2} = (\phi_i + \phi_{i\pm1})/2$.

From the cell interface extrapolated variables $\mathbf{z}_{i\pm1/2\mp}$ we recover the standard conserved and primitive variables through the equation of state. For an ideal gas, Käppeli & Mishra (2013) derive analytical expressions. In the case of a general equation of state (e.g. tabulated) a non-linear equation has to be solved to recover the conserved and primitive variables. However, this solving is very much alleviated by the fact that we have excellent initial guesses, i.e. the known cell-averaged conserved $\mathbf{u}_i$ and primitive $\mathbf{w}_i$ variables. The obtained $\mathbf{u}_{i\pm1/2\mp}$ and $\mathbf{w}_{i\pm1/2\mp}$ can then be fed into an approximate Riemann solver to obtain the numerical fluxes eq. (6).

It remains to specify the source term. For the momentum source term discretization, we follow the approach suggested by Audusse et al. (2004) for the shallow-water equations and by Botta et al. (2004) for the Euler equations and define

$$S_{\rho v,i} = \frac{p_{i+1/2-} - p_{i-1/2+}}{\Delta x} = -\int_{x_{i-1/2}}^{x_{i+1/2}} \rho \frac{\partial \phi}{\partial x} \mathrm{d}x + O(\Delta x^2). \tag{11}$$

Here the cell interface pressure $p_{i\pm1/2\mp}$ stems from the above hydrostatic reconstruction. The consistency of this momentum source term is shown by Käppeli & Mishra (2013). The energy source term is discretized by a simple centered difference expression.

Assembling all the above components, we obtain a scheme that is well-balanced for isentropic hydrostatic equilibra, i.e. the scheme is able to preserve a discrete equilibrium up to the machine precision. The generalization of the well-balanced scheme to two (3) and three dimensions as well as the extension to second order accuracy is straightforward (Käppeli & Mishra 2013).

We demonstrate the performance of the well-balanced scheme on the simulation of a three-dimensional polytrope with $\gamma = 2$. The polytrope is initialized in $[-0.65, 0.65]^3$, where its center coincides with the center of the computational domain. The detailed initial setup is described by Käppeli & Mishra (2013). First we simulate the polytrope for 20 sound crossing times with a standard and the new well-balanced scheme. The well-balanced scheme produces errors on the order of machine precision, while the standard scheme suffers from spurious deviations. This is illustrated in the left panel of figure 1. As a second test, we apply a small pressure perturbation at the center of the polytrope and simulate its evolution. The result is shown in the right panel of figure 1. As apparent from the figure, only the well-balanced scheme is able to resolve the delicate wave pattern that develops. We conclude, that the well-balanced scheme is much more efficient than the standard scheme, as a much higher resolution would be needed to obtain a comparable accuracy.

2.2. Angular momentum conserving schemes

We now show that standard Godunov-type schemes do not conserve angular momentum. Let's consider the linear momentum components of eq. (3) without gravity forces. Then the conservation law for the angular momentum density $j = x\rho v_y - y\rho v_x$ results

[2]The gravitational potential is generally a continuous (or even more regular) function.

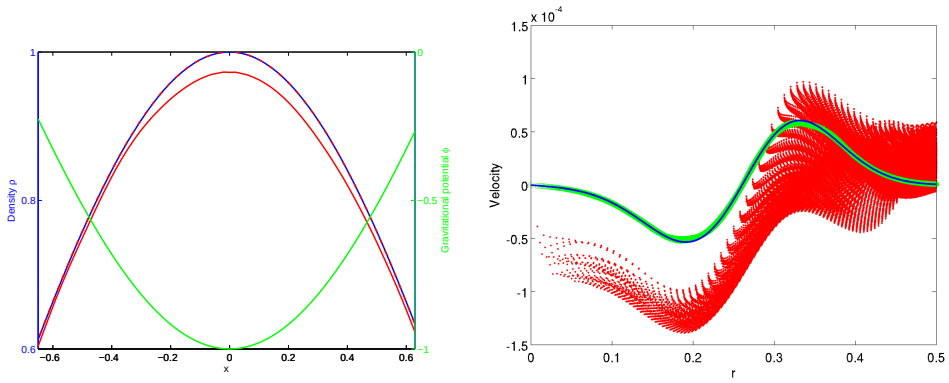

Figure 1. Three-dimensional polytrope example with $N^3 = 128^3$ cells. Left: Equilibrium preserving example. The solid blue and green lines represent the initial density and the gravitational potential profile along the x-axis with $y = z = 0$. The solid and dashed red line represent the result of a computation for 20 sound crossing times with a standard and the well-balanced schemes, respectively. Right: Scatter plot of the radial velocity for the small pressure perturbation example. The red and green dots correspond to the computation with a standard and the new well-balanced schemes, respectively. The solid blue line represents a reference solution obtained from a high resolution one-dimensional computation.

from the following elementary manipulations

$$\begin{aligned}\frac{\partial j}{\partial t} &= -x\left(\frac{\partial F^3}{\partial x}+\frac{\partial G^3}{\partial y}\right)+y\left(\frac{\partial F^2}{\partial x}+\frac{\partial G^2}{\partial y}\right)\\ &= -\frac{\partial}{\partial x}\left(xF^3-yF^2\right)-\frac{\partial}{\partial y}\left(xG^3-yG^2\right)=-F^3+G^2=0,\end{aligned}\tag{12}$$

where the F^k and G^k denote the corresponding component in the flux vectors (4). Hence, we observe that the conservation follows from the symmetry properties of the linear momentum flux tensor, i.e. $F^3 = \rho v_y v_x = \rho v_x v_y = G^2$.

Let's now repeat the above steps for a standard Godunov-type scheme eq. (5). The evolution equation for the discrete angular momentum (defined as) $j_{i,j} = x_i(\rho v_y)_{i,j} - y_j(\rho v_x)_{i,j}$ follows by

$$\begin{aligned}\frac{\mathrm{d}j_{i,j}}{\mathrm{d}t} &= -x_i\left[\frac{1}{\Delta x}\left(F^3_{i+1/2,j}-F^3_{i-1/2,j}\right)+\frac{1}{\Delta y}\left(G^3_{i,j+1/2}-G^3_{i,j-1/2}\right)\right]\\ &\quad +y_j\left[\frac{1}{\Delta x}\left(F^2_{i+1/2,j}-F^2_{i-1/2,j}\right)+\frac{1}{\Delta y}\left(G^2_{i,j+1/2}-G^2_{i,j-1/2}\right)\right]\\ &= -\frac{1}{\Delta x}\left[\left(x_{i+1/2}F^3_{i+1/2,j}-y_jF^2_{i+1/2,j}\right)-\left(x_{i-1/2}F^3_{i-1/2,j}-y_jF^2_{i-1/2,j}\right)\right]\\ &\quad -\frac{1}{\Delta y}\left[\left(x_iG^3_{i,j+1/2}-y_{j+1/2}G^2_{i,j+1/2}\right)-\left(x_iG^3_{i,j-1/2}-y_{j-1/2}G^2_{i,j-1/2}\right)\right]\\ &= -\frac{1}{2}\left(F^3_{i-1/2,j}+F^3_{i+1/2,j}\right)+\frac{1}{2}\left(G^2_{i,j-1/2}+G^2_{i,j+1/2}\right)\neq 0,\end{aligned}\tag{13}$$

where in the second equality we have used $x_{i\pm1/2} = x_i \pm \Delta x/2$ and $y_{j\pm1/2} = y_j \pm \Delta y/2$. Hence, we observe that angular momentum is only conserved if the expression after

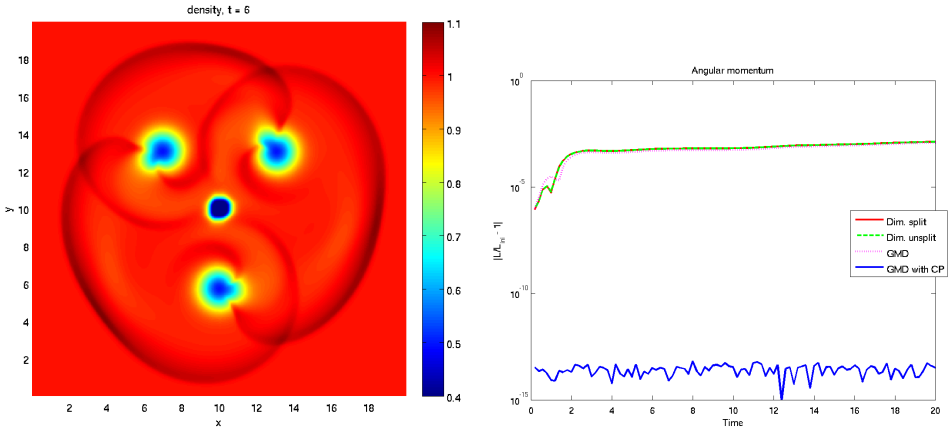

Figure 2. Three isentropic vortices and explosion test. Left: density contour. Right: total angular momentum conservation of several numerical schemes: dimensionally split (solid red), dimensionally unsplit (dashed green), genuinely multidimensional without (dashed magenta) and with constraint preservation (solid blue).

the third equality vanishes, which is generally not the case. Also note the similarity between the analytical and the discrete symmetry condition, i.e. the expression after the third equality in eq. (12) and (13).

The discrete symmetry constraint can easily be fulfilled within the framework of genuinely multidimensional schemes. We simply set the transversal momentum fluxes in both directions to $\Phi^3_{i+1/2,j+1/2} = \Psi^2_{i+1/2,j+1/2} = \chi_{i+1/2,j+1/2}$, where we define

$$\chi_{i+1/2,j+1/2} = \frac{1}{4}\left(\mathcal{F}^3_{i+1/2,j} + \mathcal{F}^3_{i+1/2,j+1} + \mathcal{G}^2_{i,j+1/2} + \mathcal{G}^2_{i+1,j+1/2}\right), \tag{14}$$

i.e. by simple averaging. More sophisticated definition are possible and this is subject of current research.

The performance of the structure preserving scheme is demonstrated on a setup involving three isentropic vortices (featuring a challenging distribution and transport of angular momentum, see figure 2 and (Yee et al. 1999)) with a strong explosion. In the right panel of figure 2 we compare the new structure preserving scheme to several standard schemes including dimensionally split, unsplit and non-constraint preserving genuinely multidimensional schemes. We observe that the new structure preserving scheme conserves angular momentum up to machine precision.

References

Audusse, E., Bouchut, F., Bristeau, M.-O., Klein, R., & Perthame, B. 2004, SIAM Journal on Scientific Computing, 25, 2050

Botta, N., Klein, R., Langenberg, S., & Lützenkirchen, S. 2004, Journal of Computational Physics, 196, 539

Käppeli, R., & Mishra, S. 2013, Well-balanced schemes for the Euler equations with gravitation, Tech. Rep. 2013-05, Seminar for Applied Mathematics, ETH Zürich

Landau, L. D., Lifschitz, E. M., & Weller, W. 1991, Lehrbuch der theoretischen Physik, 10 Bde., Bd.6, Hydrodynamik (Deutsch (Harri))

LeVeque, R. J. 2002, Finite Volume Methods for Hyperbolic Problems (Cambridge Texts in Applied Mathematics) (Cambridge University Press), 1st ed.
Mishra, S., & Tadmor, E. 2011, SIAM Journal on Numerical Analysis, 49, 1023
Yee, H., Sandham, N., & Djomehri, M. 1999, Journal of Computational Physics, 150, 199

Recent Research Reports

Nr.	Authors/Title

2013-42 S. Mishra and N. Risebro and F. Weber
Convergence rates of finite difference schemes for the wave equation with rough coeffiicients

2013-43 U. Koley and S. Mishra and N. Risebro and F. Weber
Robust finite difference schemes for a nonlinear variational wave equation modeling liquid crystals

2013-44 G. Coclite and S. Mishra and N. Risebro and F. Weber
Analysis and Numerical approximation of Brinkman regularization of two-phase flows in porous media

2013-45 M. Hutzenthaler and A. Jentzen
Numerical approximations of stochastic differential equations with non-globally Lipschitz continuous coefficients

2013-46 G. Da Prato and A. Jentzen and M. Röckner
A mild Itô formula for SPDEs

2013-47 P. Grohs and S. Keiper and G. Kutyniok and M. Schaefer
Parabolic Molecules: Curvelets, Shearlets, and Beyond

2013-48 R. Hiptmair and C. Jerez-Hanckes and C. Urzua
Optimal Operator Preconditioning for Boundary Elements on Open Curves

2013-49 P. Grohs and S. Hosseini
ε-Subgradient Algorithms for Locally Lipschitz Functions on Riemannian Manifolds

2013-50 A. Andersson and R. Kruse and S. Larsson
Duality in refined Watanabe-Sobolev spaces and weak approximations of SPDE

2014-01 M. Eigel and C.J. Gittelson and Ch. Schwab and E. Zander
A convergent adaptive stochastic Galerkin finite element method with quasi-optimal spatial meshes